RSC Advances



This is an *Accepted Manuscript*, which has been through the Royal Society of Chemistry peer review process and has been accepted for publication.

Accepted Manuscripts are published online shortly after acceptance, before technical editing, formatting and proof reading. Using this free service, authors can make their results available to the community, in citable form, before we publish the edited article. This Accepted Manuscript will be replaced by the edited, formatted and paginated article as soon as this is available.

You can find more information about *Accepted Manuscripts* in the **Information for Authors**.

Please note that technical editing may introduce minor changes to the text and/or graphics, which may alter content. The journal's standard <u>Terms & Conditions</u> and the <u>Ethical guidelines</u> still apply. In no event shall the Royal Society of Chemistry be held responsible for any errors or omissions in this *Accepted Manuscript* or any consequences arising from the use of any information it contains.



Synthesis and self-assembly of dual thermal and pH-responsive ternary

graft copolymer for sustained release drug delivery

- 3 Yinwen Li ^{a, *}, Xiuwen Zheng ^a, Kun Wu ^b, Mangeng Lu ^b
- 4 a School of Chemistry & Chemical Engineering, Linyi University, Linyi 276000, PR China.
- 5 b Guangzhou institute of Chemistry, Chinese Academy of Sciences, Guangzhou 510650, PR
- 6 China.

7

8

9

10

11

12

13

14

15

16

17

18

19

20

21

22

23

24

1

2

ABSTRACT

Ternary graft copolymer PGMA-g-(PS-r-PDMAEMA-r-POEGMA) (TGC) was prepared by a one-pot method involving the quantitative grafting of alkyne-end polystyrene (PS-C≡CH), poly[2-(dimethylamino)ethyl methacrylate] (PDMAEMA-C≡CH) and poly(oligo(ethylene glycol) methacrylate) POEGMA-C≡CH onto P(GMA-N₃) via click chemistry. TGCs selfassembled and produced stable water soluble PS-centered nano-micelles, and exhibited intriguing collapse upon proper adjustment of the solution pH and temperature. Hydrophilic Rhodamine B (RB) and hydrophobic doxorubicin (DOX) were used to investigate the encapsulation and release properties of TGCs as drug carrier. The results showed that TGCs behaved excellent loading capacities for both DOX and RB. For the hydrophilic RB, TGCs behaved two release stages, upon increasing the micelle solution pH from 7.0 to 9.0, the PDMAEMA block aggregated and caused the original stabilizing layer to aggregate and release RB firstly; while further increasing the temperature from 20 °C to 40 °C, the POEGMA block aggregated and caused the second release of RB. The rate and extent of RB release could be changed by matching the numbers of PDMAEMA and POEGMA blocks per graft copolymer. In addition, DOX was encapsulated in the hydrophobic core, upon increasing the temperature and pH, TGCs formed compact layer and inhibited DOX release.

25

Introduction

26

27

28

29

30

31

32

33

34

35

36

37

38

39

40

41

42

43

44

45

46

47

48

49

50

It is well known that amphiphilic block, graft, (miktoarm) star or hyperbranched copolymers can self-assemble into various morphologies, which depend on the selective solvent types, polymer concentrations, and chain structures. 1-6 Among them, amphiphilic graft copolymers consist of macromolecules in which one or several grafts are attached to the main polymer backbone as side chains, the grafts and backbone derive from different monomers. When two or more different types of side chains are attached to a polymer backbone to form binary, ternary, and multi-graft copolymers, and each side chain behaves like a block segment. ^{7,8} The spatial arrangement of different types of side chains along the backbone and their relative ratio dramatically affect their self-assembly behaviors, and just the mutual difference of side chains results the formation of various stable nano-type micelles, particles and aggregates. 9-14 Among the above-mentioned amphiphilic assemblies, the nano-micelles self-assembled in aqueous solution have many potential applications in biomedical fields, such as controlled drug release and gene delivery. 15-19 Taking the controlled drug release for example, polymeric micelles have attracted significant attention as ideal drug delivery systems, which are more effective to increase the apparent solubility of the hydrophobic drug and the benefit of drug, and thereby decrease the side effect. However, the burst release and instability of polymeric micelles limit the application of almost all the micelle-based drug delivery systems. 20-22 Stimuli-responsive amphiphilic copolymers have received great attention as drug nanocarriers because they can offer the advantages of improving the therapeutic activity of the drug, reducing general drug toxicity, and decreasing drug dosage. 23-28 Among them, temperature and pH-responsive mechanisms have been extensively investigated because they are relatively convenient and effective stimuli in many applications. ²⁹⁻³³ Poly(N-isopropyl acrylamide) (PNIPAAms) and poly(oligo(ethylene glycol) methacrylate) (POEGMAs) and their derivatives have been used frequently as the thermoresponsive blocks. Recently,

52

53

54

55

56

57

58

59

60

61

62

63

64

65

66

67

68

69

70

71

72

73

74

75

poly[oligo (ethylene glycol) methacrylate]s (POEGMAs) were reported to possess similar or even superior thermosensitivity than PNIPAAms, and the biocompatibility of POEGMAs is also excellent and attractive. ¹⁴ Poly[2-(dimethylamino) ethyl methacrylate] (PDMAEMA), Poly[(diethylamino) ethyl methacrylate)] (PDEAEMA) and poly(4-vinylpyridine) (PVP) are well known as the pH-responsive polymers, and they behave water-insoluble and soluble due to protonation of tertiary amine residues as the pH changed. These copolymers have potentially biomedical and biotechnology applications since they are mainly composed of biocompatible segments. Moreover, dual responsive polymeric nanoaggregate is a much more attractive topic and receiving wide and intensive interest due to its potential advantage in achieving much better release and control compared to mono-responsive nanocarriers. Up to present, a series of smart nanoparticles were prepared based on the block, star and hyperbranched copolymer which behave dual thermo- and pH- sensitive properities.³⁸⁻⁴⁷ For further reducing unwanted side effects of existing drugs as well as enriching the drug candidates, herein, we present a facile method for preparing dual thermo- and pH- responsive nanoparticles based on a novel functional ternary graft copolymer, PGMA-g-(PS-r-PDMAEMA-r-POEGMA) (TGC), which is shown in Scheme 1. The graft-onto method was used to produce the desired ternary graft copolymer. The backbone polymer was the poly (3azido-2-hydroxypropyl methacrylate), P(GMA-N₃)₅₀. The grafts used were water insoluble alkyne-end polystyrene (PS-C≡CH) and water soluble poly[(2-(dimethylamino) ethyl methacrylate)] (PDMAEMA-C≡CH) and poly (MEO₂MA-co-OEGMA) (POEGMA-C≡CH), respectively. The precursory grafts PS-C=CH, PDMAEMA-C=CH and POEGMA-C=CH were coupled to P(GMA-N₃)₅₀ via Cu catalyzed alkyne-azide cycloaddition.⁴⁸ According to our experiment, the (-C \equiv CH) to (N₃) molar ratio was determined to 30/100-40/100, and the residual N₃ groups were deactivated by reaction with propargyl alcohol. The results showed that TGCs exhibited excellent intriguing dual responsive phase transition behavior in aqueous

- solution by changing solution pH and temperature. The nano-micelles prepared by TGCs have
- been used as drug delivery vehicles, and behaved as controlled two-stage drug release.

Experimental section

Materials

Styrene (St), 2-(dimethylamino) ethyl methacrylate (DMAEMA), 2-(2-methoxyethoxy) ethyl methacrylate (MEO₂MA)(Mn, 188 g mol⁻¹), oligo(ethylene glycol) methyl ether methacrylate (OEGMA) (Mn, 475 g mol⁻¹) were all analytical grade, acquired from TCI, Japan and passed through short basic alumina column before use. Pentamethyldiethylenetriamine (PMDETA, analytical grade) was purchased from Aladdin, China. Rhodamine B (RB, ≥97%) was acquired from Aladdin, China, Doxorubicin hydrochloride (DOX·HCl, ≥99%) was purchased from Dalian Meilun Biotechnology Co., Ltd., China, and their molecular structures are shown in Scheme 2. Cyclohexanone, Diphenyl ether, Tetrahydrofuran (THF), Dichloromethane (CH₂Cl₂), Diethyl ether, Dimethylformamide (DMF) and Hexane were all analytical grade and used as received from Sinopharm Chemical Reagent. Co., Ltd, China. The alkynyl-end ATRP initiator (2-alkyne 2-bromoisobutyrate, ABIB), 2-methoxyethyl 2-bromoisobutyrate (MBIB) and poly (3-azide-2-hydroxypropyl methacrylate) (P(GMA-N₃)) used in this project were prepared according to our previously reported procedure.⁸

Synthesis of PS-C≡CH

PS-C≡CH was synthesized by the ATRP of St monomer using ABIB as the initiator. A typical procedure is described as follows: the schlenk tube was purged with dry argon for 30 minutes, a degassed mixture of St (1.04 g, 10 mmol), toluene (5 g), ABIB (0.0276g, 0.1 mmol) initiator and copper bromide (0.0143 g, 0.1 mmol) was added to a schlenk tube, degassed via three freeze-thaw-pump cycles and back-filled with argon. Then PMDETA (0.035 g, 0.2 mmol) were added. The mixture was heated at 80 °C in an oil bath for 6 h. The experiment was stopped by immersing the tube into liquid nitrogen and then exposing the contents to air. The

102

103

104

121

122

123

124

125

- final mixture was diluted in CH₂Cl₂ and passed through a short neutral alumina column in order to remove copper catalyst. Then the filtrate was subsequently added into 500 mL of hexane to precipitate, and the precipitate was dried under vacuum for 12 h to get white powder. Yield: $\approx 47.7\%$. ¹H NMR (400 MHz, CDCl₃, δ): 6.17 \sim 7.21 (5H, $-C_6H_5$), 4.12-4.30 (-
- 105 O- CH_2 -, 2H), 1.2~2.1 (3H, - $CHCH_2$ -), 0.85~1.04 (6H, -(CH_3)₂).

106 **Synthesis of PDMAEMA-C≡CH**

107 PDMAEMA-C≡CH was synthesized by the ATRP of DMAEMA monomer using ABIB as 108 the initiator. A typical procedure is described as follows: the schlenk tube was purged with 109 dry argon for 30 minutes, a degassed mixture of DMAEMA (1.57g, 10 mmol), ethanol (5 g), 110 ABIB (0.0276g, 0.1 mmol) initiator and copper bromide (0.0143 g, 0.1 mmol) was added to a 111 schlenk tube, degassed via three freeze-thaw-pump cycles and back-filled with argon. Then 2, 112 PMDETA (0.035 g, 0.2 mmol) were added. The mixture was heated at 40 °C in an oil bath for 113 6 h. The experiment was stopped by immersing the tube into liquid nitrogen and then 114 exposing the contents to air. The final mixture was diluted in CH₂Cl₂ and passed through a 115 short neutral alumina column (200 mesh) in order to remove copper catalyst. Then the filtrate was subsequently added into 500 mL of hexane to precipitate, and the precipitate was dried 116 under vacuum for 24 h to get white powder. Yield: ≈40.3%. ¹H NMR (400 MHz, CDCl₃, δ): 117 118 4.01-4.12 (2H, $-COCH_2$ -), 2.50-2.59 (2H, $N-CH_2$ -), 2.20-2.30 (6H, $-N(CH_3)_2$), 1.80-1.91 (2H, 119 $-CH_2$ -C-), 1.8-2.0 (2H,-C H_2 -), 0.85-1.04 (3H, -C H_3).

120 **Synthesis of POEGMA-C≡CH**

POEGMA-C≡CH was synthesized by the ATRP of MEO₂MA and OEGMA monomers using ABIB as the initiator. A typical procedure is described as follows: the schlenk tube was purged with dry argon for 30 minutes, a degassed mixture of MEO₂MA (1.88g, 9.5 mmol) MEO₂MA (0.24 g, 0.5 mmol), ethanol (5 g), ABIB (0.0276g, 0.1 mmol) initiator and copper bromide (0.0143 g, 0.1 mmol) was added to a schlenk tube, degassed via three freeze-thaw-

pump cycles and back-filled with argon. Then 2, 2- bipyridyl (0.312 g, 0.2 mmol) were added.
The mixture was heated at 60 °C in an oil bath for 4 h. The experiment was stopped by
immersing the tube into liquid nitrogen and then exposing the contents to air. The final
mixture was diluted in CH_2Cl_2 and passed through a short neutral alumina column (200 mesh)
in order to remove copper catalyst. Then the filtrate was subsequently added into 500 mL of
hexane to precipitate the polymer, and the precipitated viscous solid was dried under vacuum
for 24 h. Yield: \approx 52.8%. ¹ H NMR (400 MHz, CDCl ₃ , δ): 4.70-4.75 (CHC-C H_2 -O-), 3.31-4.12
(-(CH ₂ -CH ₂ -O)n-CH ₃), 2.24-2.35 (CHC-), 1.80-1.89 (2H,-CH ₂ -), 0.84-1.47 (-CH ₃).

Synthesis of ternary graft copolymers (TGCs)

In an example preparation, DMF (16.0 mL), P(GMA-N₃)₅₀ (0.086 g, 50 mmol of azide groups), PS-C \equiv CH (0.245 g, 5 mmol of alkyne groups), PDMAEMA-C \equiv CH (0.315 g, 5 mmol of alkyne groups), POEGMA-C \equiv CH (0.53g, 5 mmol of alkyne groups) and an aqueous sodium ascorbate solution (0.1 g, 50 mmol, dissolved into 0.20 mL of water) were mixed in a 50 mL round-bottomed flask and deoxygenated via bubbling with argon for 50 min. Then, an saturated aqueous solution of CuSO₄ ·5H₂O (0.40 ml) was added. This was followed by stirring the reaction mixture at 50 °C for 72 h. Subsequently, degassed propargyl alcohol (0.20 g) was injected into the flask, and the reaction mixture was stirred for 24 h to deactivate the residual azide groups. The experiment was stopped by exposing the catalyst to air, then the final mixture was diluted with DMF and subsequently purified by dialysis in aqueous 5% EDTA solution (molar mass cut off: 14000), finally purified by dialysis in aqueous solution for 48h, and freeze-dried in vacuum TGC was obtained as light yellow solid in a 67.1% yield.

Characterization

FT-IR spectra were recorded on a Nicolet 5100 spectrometer. ¹H NMR spectra were obtained on a Bruker DMX-400 spectrometer. The number average molar mass (Mn) and dispersity index (Mw/Mn, DI) were determined using a Waters 1515 size exclusion chromatography (SEC) system equipped with a Waters 2414 refractive index (RI) detector. The SEC system

was equipped with a guard column in addition to styragel HR₃ and HR₄ columns, which were calibrated using monodispersed PS standards and DMF solution as eluent.

The cloud point were determined by UV-vis spectroscopy (U-3010 Spectrophotometer), and the transmittance of polymeric aqueous solutions (0.2 mg mL⁻¹) was recorded at temperatures ranging from 20 °C to 45 °C. The cloud point at specific concentration was determined as the temperature corresponding to 10% decrease of the optical transmittance. The hydrodynamic diameters (Dh) of the micelles and their polydispersity indices (PDI) were determined by dynamic light scattering (DLS) on a Malven Zetasizer Nano System (Nanozs90). The morphology and architecture of nano-sized aggregates were visualized by transmission electron microscopy (TEM), and the samples were prepared by placing polymer aqueous solution on copper grids in a biochemical incubator thermostatted at 25 °C or 50 °C, and stained with phosphotungstic acid before observation on a JEM-100CX II microscope operated at 80 kV. The samples were fixed onto the surface of an AFM-holder, and the surface morphologies of the samples were observed using a Multimode 8 SPM AFM system (Bruker, USA) using the ScanAsyst TM mode.

Micelles preparation

In a typical example, 10 mg of TGC₁ was dissolved in DMF (1.0 mL) and stirred for at least for 24 h, and then under vigorous stirring, 10 ml deionized water was added slowly at a flow rate of 0.2 mL min⁻¹ until the appearance of the solution with a characteristic bluish tinge. After the addition was completed, the dispersion was left stirring for another 48 h at room temperature, and DMF was removed by dialysis against deionized water. Aqueous solution with light bluish tinge was typically obtained.

The pKas of TGCs were titrated as follows: First, the pH value of TGC polymer solution (1 mg mL⁻¹) was adjusted with hydrochloric acid (HCl) to strong acid state (pH≈2); then, the pH values of the TGC polymer solution (1 mg/mL) were titrated by a standard base solution (NaOH, pH=13.0) under continuous stirring using a PH 211 Microprocessor pH meter

(HANNA instruments, Italy). The acid-base titration curves about the pH value to base volume (mL) were drawn, and the pKas were calculated by pKa=pH+ $Log[(1-\alpha)/\alpha]$, in other word, the pKas were calculated as the pH at 50% ionization.

In vitro drug loading and release

178

179

180

181

182

183

184

185

186

187

188

189

190

191

192

193

194

195

196

197

198

199

200

201

202

The TGC₁ (50.0 mg) in 5.0 mL of DMF was mixed with 50.0 mg of RB or DOX (neutralized with one molar equivalent of triethylamine). The mixture was allowed to stand at room temperature for 24 h. Then, 5 mL of deionized water was added dropwise to this solution under stirring. The mixture was stirred at room temperature for another 48 h, and the organic solvent was removed by dialysis against deionic water for 24 h to obtain the drug loaded micelles. The solution was filtered and freeze-dried. The drug loading efficiency (DLE %) of drug-loaded micelles were calculated by the following equations: DLE (%) = (M_I/M_0) $\times 100$ %. where M_I is the amount of drug in micelle and M₀ is the total amount of drug for drug loading. In vitro drug release behaviors from the micelles were investigated in PBS buffer solution. The weighed freeze-dried drug-loaded micelles were suspended in 5 mL of PBS with pH=7.0. and introduced into a dialysis bag (molar mass cut off: 3500). We initiated the release experiment by placing the end-sealed dialysis bag in 60 mL PBS with pH=9.0 at 20 °C with continuous shake at 70 rpm. At predetermined intervals, 1 mL of drug release solution was taken out, and an equal volume of fresh PBS with pH=9.0 was replenished. The amount of released drug solution was assayed by spectrophotometry using the standard curve method. After the drug release reached the equilibrium, the dialysis bag was transferred into the PBS solution with pH=9.0 at 40 °C, At predetermined intervals, 1 mL of drug release solution was

Results and discussion

taken out, and an equal volume of fresh PBS with pH=9.0 was replenished. The amount of

released drug solution was assayed by spectrophotometry using the standard curve method.

205

215

226

227

Synthesis	of	monomers	and	ternary	graft	copolymer	S
Symulations	O.	inonomici 5	unu	cci iidi y	Simil	coporymer	S

204 The alkynyl-end ATRP initiator (ABIB), 2-methoxyethyl 2-bromoisobutyrate (MBIB) and poly (3-azide-2-hydroxypropyl methacrylate) (P(GMA-N₃)) were prepared according to our previously reported procedure.⁸ PS-C≡CH, PDMAEMA-C≡CH and POEGMA-C≡CH were 206 207 first synthesized, and then the three polymers were grafted onto the P(GMA-N₃) backbone to 208 yield PGMA-g-(PS-r-PDMAEMA-r-POEGMA) copolymers (TGCs). Scheme 2 shows the 209 reactions used to prepare the individual components and the final graft copolymers. 210 According to Scheme 2, PS-C≡CH, PDMAEMA-C≡CH and POEGMA-C≡CH were 211 synthesized in two steps. First, reacting propargyl alcohol with 2-bromoisobutyric bromide 212 following our previous report yielded propargyl 2-bromoisobutyrate (ABIB). The latter was 213 then used to initiate St, DMAEMA, and MEO₂MA and OEGMA to yield PS-C≡CH, 214 PDMAEMA-C=CH and POEGMA-C=CH. DMAEMA and (MEO₂A-co-OEGMA) polymerization using ABIB as initiator were firstly reported. When the mole ratio of 216 [monomer]₀/[initiatoir]₀/[CuBr]₀/[ligand]₀ was 100/1/1/2, it was found that the well-defined 217 polymer was easily produced. The resultant PDMAEMA-C≡CH and POEGMA-C≡CH were characterized by FT-IR and ¹H NMR, and shown in Fig. 1 and Fig. 2. On the basis of ¹H 218 219 NMR result, comparing the peak area of the initiator's methylene protons (HC \equiv C-C H_2 -) at 220 4.66 ppm with those of the methyl groups of the -N(CH₃)₂ of DMAEMA at 2.10 ppm yielded 221 a repeat unit number (actual DP) of 39. For POEGMA-C≡CH, based on the ¹H NMR result, 222 by calculating the ratio both the area of the chemical shift of 4.71 ppm of HC \equiv C-C H_2 - for 223 ABIB and that of 3.34 ppm of CH_3 -O- for POEGMA, the actual DP of OEGMA was 47. 224 PGMA-g-(PS-r-PDMAEMA-r-POEGMA) was synthesized by coupling P(GMA-N₃) with 225 PS-C=CH, PDMAEMA-C=CH, and POEGMA-C=CH. TGCs were started by one-pot graft

reaction of PS-C≡CH, PDMAEMA-C≡CH, and POEGMA-C≡CH onto P(GMA-N₃) for 72 h, and followed by another 24 h with an excess of propargyl alcohol to exhaust the residual azide groups. Two ternary graft copolymers denoted as TGC_1 and TGC_2 were prepared by grafting various ratios of PDMAEMA-C \equiv CH and POEGMA-C \equiv CH. The feed molar ratios used to prepare the copolymers and the molecular characteristics are listed in Table 2.

Table 1. Preparation conditions and molecular characteristics of the precursory polymers

	$[M_0]/\left[I_0\right]^b$	Yield ^c	NMR	NMR	SEC	SEC
Sample ^a		(%)	DP^d	M n e (kg/mol)	$Mn^f(kg/mol)$	M w $/M$ n f
P(GMA-N ₃) ₅₀	-	91.4	51	8.6	12.7	1.27
PS-C≡CH	100:1	47.7	45	4.9	5.0	1.04
PDMAEMA-C≡CH	100:1	40.3	39	6.3	6.7	1.09
POEGMA-C≡CH	100:1	52.8	47	10.6	11.9	1.12

^a PS-C \equiv CH, PDMAEMA-C \equiv CH and POEGMA-C \equiv CH were prepared through the ATRP. ^b

The molar feed ratio is denoted as $[M]/[I]_0/[CuBr]_0/[L]_0$. Yield was evaluated by the gravimetric method. The DPs were evaluated via 1H NMR. e Mn was evaluated via 1H NMR.

^f Mn and Mw/Mn were evaluated by SEC using DMF as the eluent and PS standards.

TGCs were analyzed by SEC, FT-IR and ¹H NMR. Fig. 3 compared the SEC traces of the precursors exclude PS-C≡CH, PDMAEMA-C≡CH, POEGMA-C≡CH and TGC₂. An important result of Fig. 3 was that no SEC peaks for the precursors were observed using the recipes shown in Table 2. This was due to the low molar ratios used for the polymer alkyne to azide groups used during the reactions. As listed in Table 2, the highest molar ratio used between PS-C≡CH,PDMAEMA-C≡CH, and POEGMA-C≡CH and the azide groups of P(GMA-N₃) was 40%, therefore, almost all the PS-C≡CH, PDMAEMA-C≡CH, and POEGMA-C≡CH were reacted absolutely with P(GMA-N₃).

The FT-IR and ¹H NMR spectra of TGC₂ are shown in Fig. 4. The azide peak at 2104 cm⁻¹ totally disappeared, and compared with P(GMA-N₃)₅₀, the intensity of the peak at 1680 cm⁻¹ increased obviously. Moreover, all the protons of the grafted PS, PDMAEMA and POEGMA

chains were observed in the spectrum measured in DMSO, and the signals at 7.9 ppm for the protons of the triazole linkage in the spectrum was also appeared. These peaks provided direct evidence for the desired click chemistry.

Table 2. Preparation conditions and molecular characteristics of binary graft copolymers

Sample	Feed molar	$M_{\rm n}({}_{ m theory})$	$M_{\rm n}({}_{ m SEC}{}^b)$	M w/ M n b	Cloud point ^c
	ratio[(N ₃): $(-C \equiv CH]^a$	(kg/mol)	(kg/mol)	(DI)	(°C)
TGC ₁	50:5:5:5	74.5	89.2	1.29	38.4
TGC_2	50:5:5:10	84.3	105.4	1.30	39.2

 $a = N_3$: $[x_{(PS-C=CH)}]$: $[y_{(PDMAEMA-C=CH)}]$: $[z_{(POEGMA-C=CH)}]$. b = Mn, theory $= Mn(P(GMA-N_3)) + Mn$

 $x \times n \times 4900 + y \times n \times 6300 + z \times n \times 10600$; ^bMolar mass and distributions ($_{Mw}$ / $_{Mn}$, DI) were determined by SEC using DMF as eluent relative to polystyrene standards; ^cMeasured with a concentration of 0.2 mg mL⁻¹, temperature increase at 1 °C min⁻¹ by UV-vis spectroscopy.

Self-assembly behaviors of TGCs

It was anticipated that the obtained TGCs were amphiphilic because of the hydrophobic PS blocks and the hydrophilic POEGMAs and PDMAEMA blocks. Hence, the amphiphilic TGCs formed micelles in water and the self-assembly behaviors in aqueous solution were investigated using fluorescence spectroscopy, DLS, and TEM.

Pyrene as a fluorescence probe has very low fluorescence intensity in aqueous solution due to its hydrophobic nature, and the fluorescent intensity increases significantly once it is transferred into a hydrophobic environment. Fig. 5(a) shows the change in the fluorescent intensity of pyrene as a function of the concentration of TGC solutions. As known, pyrene is very sensitive to the chemical environment, the fluorescence intensity of pyrene is almost constant at low concentration of TGC, and above a certain concentration, the intensity increases dramatically, indicating the transfer of pyrene into a hydrophobic environment. Such a sudden change of the fluorescent intensity indicated the formation of micelle from

TGC at this concentration. This concentration can be defined as the critical micelle
concentration (CMC), and the CMC was obtained from the plot of fluorescence intensity ratio
of I_{395}/I_{385} versus the concentration of TGCs. The CMC value of TGC ₂ was determined to be
0.082 mg/mL.
Owing to the presence of POEGMA and PDMAEMA grafts for TGCs, the micelles were
assessed to have dual thermo- and pH-sensitive properties. 49-51 When the temperature and pH
were changed to a certain level, the micelles started to aggregate and the solution became
cloudy, therefore, DLS and TEM were used to determine the stimuli induced size changes of
the micelles. Fig. 6 shows the results of the DLS measurements of the micelle of TGC ₂ (0.2
mg mL ⁻¹) with temperature and pH at 20 °C and pH=7, 40 °C and pH=7, 20 °C and pH=9, 40
°C and pH=9. The hydrodynamic radius (Rh) of the TGC ₂ was measured to decrease from
167.5 nm at 25 °C and pH= 7 to 76.4 nm at 40 °C and pH= 7. The decrease in Rh could be
attributed to the hydration to dehydration process of the POEGMA and PDMAEMA chains in
the shell with the temperature increase, and the polydispersity index (PDI) decreased from
0.77 to 0.21, indicating relatively more uniform nano-aggregates were formed.
pH-sensitive PDMAEMA block was also introduced into TGCs, therefore, when changes
the pH of TGC micelles, its hydrodynamic radii also changed. For TGC ₂ micelles at 20 °C,
while changed the pH, the hydrodynamic radius (Rh) of the TGC ₂ decreased from 167.45 nm
at 20 °C with pH=7 to 92.6 nm at 20 °C with pH=9. The decrease in Rh was also attributed to
the rapid hydration to dehydration process of the PDMAEMA chains in the shell with the pH
increase, and the polydispersity index (PDI) also decreased from 0.77 to 0.33. While
increased the temperature and pH jointly to 40 °C and pH=9, the hydrodynamic radius (Rh) of
the TGC ₂ decreased to 30.9 nm with PDI of 0.09. The significantly decrease in Rh was
attributed to the rapid hydration to dehydration process of the POEGMAs and PDMAEMA
chains in the shell, indicating more uniform small nano-aggregates formed.

To further examine visually the size and morphology of TGCs, the typical TEM image of TGC₂ is presented in Fig. 7. Solid spheres were clearly observable in the TEM images, and the Z-average diameter (DZ) was about 102 nm at 20 °C with pH=7. The formation of spheres could be attributed to the difference in hydrophobic properties in TGCs molecules, PS block and PGMA backbone are highly hydrophobic, and PDMAEMA and POEGMA chains possess plenty of hydrophilic groups. In order to minimize the system energy of the complex of TGCs, PS molecules located in the inner part of the complex, and spontaneously formed solid spheres. Moreover, TGCs behaved thermo- and pH-responsive behaviors, when increase its temperature and pH, it was found obviously that TGCs could self-assemble into more evenly nano-sized aggregates, the basically uniform aggregates formed with DZ of 20-50 nm.

Drug loading and release

In aqueous solution, stable micelles can be easily formed for TGCs with hydrophobic PS as the core, and POEGMAs and PDMAEMA as hydrophilic shell. A hydrophobic drug, DOX and a hydrophilic guest, RB were used to be loaded into the TGCs micelles and studied the release property. The results of the DOX encapsulation experiment are shown in Fig. 8. DOX is an anti-cancer drug, which has a low solubility in water and dichloromethane. As shown in Fig. 8(c), when adding water to the mixture of DOX/dichloromethane, only few DOX transferred from dichloromethane into to the water phase. While TGC₂ micelle solution was added into the mixture of DOX/dichloromethane, as shown in Fig. 8(d) and (e), it was found that TGC micelle was effective to encapsulate DOX, and DOX was completely transferred from dichloromethane into to the TGC micelles, when TGC₂ micelle concentration was increased from 0.2 mg mL⁻¹ to 1.0 mg mL⁻¹.

TGCs display thermally-responsive behavior meaning that POEGMAs and PDMAEMA segments are soluble in aqueous solution at low temperature below their cloud points but can be dehydrated and aggregated when TGCs are heated above their cloud point. The cloud point

was determined by UV-vis spectroscopy and determined as the temperature corresponding to
10% decrease in the optical transmittance. The cloud point for TGC_1 and TGC_2 were 38.4 $^{\circ}C$
and 39.2 °C, separately. Meanwhile, PDMAEMA segment also endows TGCs with pH-
sensitivity. The acid-base titration curves indicated that the pKas were equal to the pH at
50% ionization, and the pKas for TGC ₁ and TGC ₂ were 7.81 and 7.89, separately. Therefore,
when the external stimulations (temperature or pH) change, POEGMAs or PDMAEMA
segments dehydrate and aggregate, and result in the release of entrapped drugs.
To test the possible use of this kind of TGC micelles as drug carriers, DOX and RB were
loaded into the micelles and the release behaviors were studied. 19, 31 The results of the DOX
and RB load and release experiments are shown in Fig. 9 and Fig. 10. The DLE (%) was
depended on the compositions of TGCs, for DOX, the DLE (%) were 46.8 % and 48.5% for
TGC ₁ and TGC ₂ micelles (1 mg mL ⁻¹), respectively; Similar results were obtained for Rh, the
DLE (%) were 61.2 % and 75.1% for TGC ₁ and TGC ₂ micelles (1 mg mL ⁻¹), respectively.
The difference for the DLE% of the TGCs loaded DOX and RB was determined by the core-
shell structure of the TGCs. The hydrophobic DOX was encapsulated by hydrophobic core
formed by hydrophobic segment of TGCs, while the hydrophilic RB was encapsulated by
hydrophilic shell formed by hydrophilic segment of TGCs. It could be inferred that the
micelle formed from TGCs had relative large hydrophilic shell and small hydrophobic core.
Therefore, the micelles formed from TGCs encapsulated much more Rh in the hydrophilic shell
than DOX in the hydrophobic core. Although TGCs showed excellent loading capacities for
both DOX and RB, in release experiment, it was found that only less than 10% DOX was
released out for about 48 h. This was mainly due to the hydrophobic DOX was encapsulated
in hydrophobic core of TGC micelles, when the temperature or pH changed, temperature-
sensitive POEGMAs or pH-sensitive segments dehydrated, aggregated, and created a more
compact shell closely around the periphery, thereby prevented the effective release of DOX

344

345

346

347

348

349

350

351

352

353

354

355

356

357

358

359

360

361

362

363

364

365

366

While for hydrophilic RB, The release behaviors were first studied at pH=9.0 and 20 °C. As shown in Fig. 10, it was interesting to note that the RB release behaved two stage release process. When changed the pH from 7.0 to 9.0, the release was called the stage I, and then when the temperature rose from 20 °C to 40 °C, the release was called stage II. For TGC₁ micelles, about 25 % of the loaded Rh was released for 48 h in the stage I, and about 37 % of the loaded RB was released in the stage II. While for TGC₂ micelles, similar release result was obtained, about 30 % of the loaded RB was released for 48 h in the stage I, and about 46 % of the loaded RB was released in the stage II. It was interesting to observe that the both TGC₁ and TGC₂ micelles all showed excellent release capacities, but the release of TGC₁ was obviously lower than that of TGC₂ in both stage I and II. Although TGCs had similar molecular structure, there were indeed existed differences for TGC₁ and TGC₂ with different branched POEGMAs. As shown in table 2, for TGC₂, the POEGMAs content increased obviously, the hydrophilic POEGMAs, the more drugs were loaded. Therefore, for release process, TGCs with more hydrophilic POEGMAs

TGCs are shown in scheme 4.

Conclusions

In summary, Ternary graft copolymer PGMA-g-(PS-r-PDMAEMA-r-POEGMA) (TGC) was prepared by grafting of alkyne-end PS-C=CH, PDMAEMA-C=CH and POEGMA-C=CH onto P(GMA-N₃) via click chemistry. The self-assembly behaviors were investigated by combination of Fluorescence spectroscopy, DLS and TEM, and the results indicated that TGCs self-assembled and produced stable soluble PS-centered nano-micelles. Moreover,

behaved much more drugs release. This results indicated that the release capacities were

mainly dependent on the polymer molecular structures of TGCs. The schematic illustrations

of dual thermo- and pH-induced self-assembly and possible loading and release behaviors for

- TGC exhibited intriguing dual collapse upon proper adjustment of the solution pH and temperature, and Hydrophobic doxorubicin (DOX) and hydrophilic Rhodamine B (RB) were used as model drugs to investigate the encapsulation and release properties of TGCs as drug carrier. The results showed that TGCs behaved excellent loading capacities for both DOX and RB. While in release experiment, only less than 10% DOX was released out which indicated that DOX was encapsulated in hydrophobic core, temperature- and pH-sensitive segments dehydrated, aggregated, and created a more compact shell and prevented the effective DOX release. For hydrophilic RB, TGC behaved two release stages. Upon increasing the pH from 7.0 to 9.0, the PDMAEMA block aggregated and caused the first release of RB, when further increasing the temperature from 20 °C to 40 °C, the POEGMA block aggregated and caused the second release. The rate and extent of RB release could be changed by matching the numbers of PDMEA and POEGMA blocks per graft copolymer.
- 379 Acknowledgements
- 380 The authors appreciate the Natural Science Foundation of China (No. 21405074), and
- 381 National undergraduate training programs for innovation and entrepreneurship (No.
- 382 201410452006).

368

369

370

371

372

373

374

375

376

377

378

383 **REFERENCES**

- 384 (1) Y. Y. Mai, A. Eisenberg, Chem. Soc. Rev., 2012, 41, 5969-5985.
- 385 (2) R. A. Ramli, W. A. Laftah, S. Hashim, RSC Adv., 2013, 3, 15543-15565.
- 386 (3) S. S. Sheiko, B. S. Sumerlin, K. Matyjaszewski, Prog. Polym. Sci., 2008, 33, 759-785.
- 387 (4) Wyman, I. Njikang, G. Liu, G. J. Prog. Polym. Sci., 2011, 36, 1152-1183.
- 388 (5) X. B. Zhao, P. Liu, ACS Appl. Mater. Interfaces, 2015, 7, 166-174.
- 389 (6) K. Miao, H. H. Liu, Y. L. Zhao. Thermo, pH and reduction responsive coaggregates
- comprising AB2C2 star terpolymers for multi-triggered release of doxorubicin. Polym.
- 391 Chem. 2014,5, 3335-3345.

- 392 (7) F. Liu, J. W. Hu, G. J. Liu, C. M. Hou, S. D. Lin, H. L. Zou, G. W. Zhang, J. P. Sun, H. S.
- 393 Luo, Y. Y. Tu, Macromolecules, 2013, 46, 2646-2657.
- 394 (8) Y. W. Li, X. W. Zheng, H. Y. Zhu, K. Wu, M. G. Lu, RSC Adv., 2015; 5, 46132-46145.
- 395 (9) S. Chantasirichot, Y. Inoue, K. Ishihara, Macromolecules, 2014, 47, 3128-3135.
- 396 (10) J. Jin, D. X. Wu, P. C. Sun, L. Liu, H. Y. Zhao, Macromolecules, 2011, 44, 2016-2024.
- 397 (11) Z. P. Cheng, X. L. Zhu, E. T. Kang, K. G. Neoh, Langmuir, 2005, 21, 7180-7185.
- 398 (12) D. Kakkar, S. Mazzaferro, J. Thevenot, C. Schatz, A. Bhatt, B. S. Dwarakanath, H. Singh,
- 399 A. K. Mishra, S. Lecommandoux, Macromol. Biosci., 2015, 15, 124-137.
- 400 (13) A. Heise, J. L. Hedrick, C. W. Frank, R. D. Miller, J. Am. Chem. Soc., 1999, 121, 8647-
- 401 8648.
- 402 (14) Y. W. Li, H. L. Guo, Y. F. Zhang, J. Zheng, J. Q. Gan, X. X. Guan, M. G. Lu, RSC Adv.,
- 403 2014, 4, 17768-17779.
- 404 (15) Y. Zhao, F. Sakai, L. Su, Y. J. Liu, K. C. Wei, G. S. Chen, M. Jiang, Adv. Mater., 2013,
- 405 25, 5215-5256.
- 406 (16) Z. Ahmad, A. Shah, M. Siddiqa, H. B. Kraatz, RSC Adv., 2014, 4, 17028-17038.
- 407 (17) F.J. Xu, W.T. Yang, Prog. Polym. Sci., 2011, 36, 1099-1131.
- 408 (18) L. Zhang, Y. C. Li, J. C. Yu, J. Mater. Chem. B, 2014, 2, 452-470.
- 409 (19) W. Wang,; J. X. Ding, C. S. Xiao, Z. H. Tang, D. Li, J. Chen, X. L. Zhuang, X. S. Chen,
- 410 Biomacromolecules, 2011, 12, 2466-2474.
- 411 (20) C. L. Lo, C. K. Huang, K. M. Lin, G. H. Hsiue, Biomaterials, 2007, 28, 1225-1235.
- 412 (21) J. Liu, C. Detrembleur, S. Morne, C. Jerome, E. Duguet, J. Mater. Chem. BDOI:
- 413 10.1039/c5tb00664c.
- 414 (22) O. G. Schramm, M. A. R. Meier, R. Hoogenboom, H. P. van Erp, J. F. Gohyac, U. S.
- 415 Schubert, Soft Matter, 2009, 5, 1662-1667.

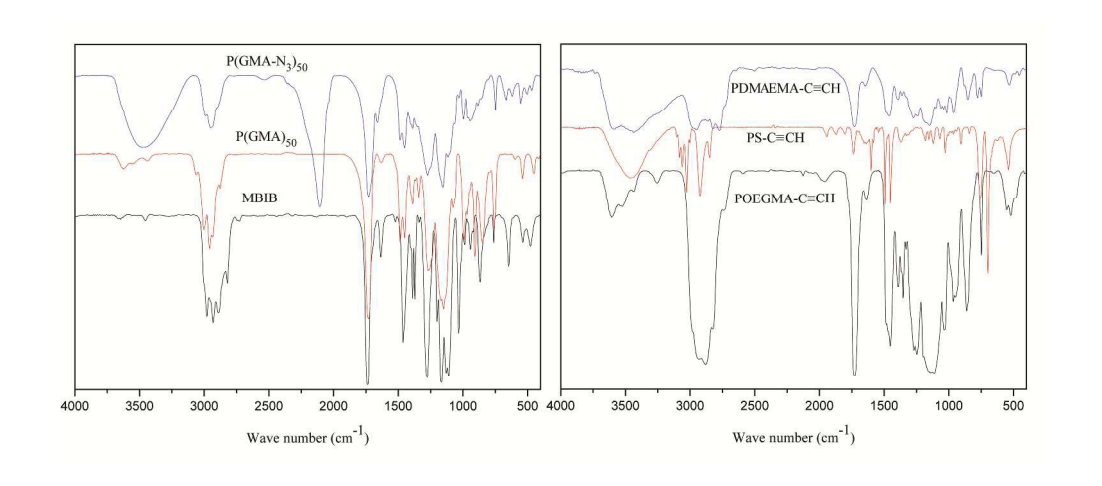
- 416 (23) R. J. Dong, Y. F. Zhou, X. H. Huang, X. Y. Zhu, Y. F. Lu, J. Shen, Adv. Mater., 2015,
- 417 27, 498-526.
- 418 (24) W. N. Xu, I. Choi, F. A. Plamper, C. V. Synatschke, A. H. E. Müller, Y. B. Melnichenko,
- 419 V. V. Tsukruk, Macromolecules, 2014, 47, 2112-2121.
- 420 (25) W. D. Zhang, W. Zhang, Z. B. Zhang, Z. P. Cheng, Y. F. Tu, Y. S. Qiu, X. L. Zhu, J.
- 421 Polym. Sci. Part A: Polym. Chem., 2010, 48, 4268-4278.
- 422 (26) F. Liu, M. W. Urban, Prog. Polym. Sci., 2010, 35, 3-23.
- 423 (27) Y. Zhang, H. F. Chan, K. W. Leong, Adv. Drug Deliv. Rev., 2013, 65, 104-120.
- 424 (28) A. K. Bajpai, S. K. Shukla, S. Bhanu, S. Kankane, Prog. Polym. Sci., 2009, 33, 1088-
- **425** 1118.
- 426 (29) C. Weber, R. Hoogenboom, U. S. Schubert, Prog. Polym. Sci., 2012, 37, 686-714.
- 427 (30) Y. W. Li, H. L. Guo, J. Zheng, J. Q. Gan, Y. Zhang, X. X. Guan, K. Wu, M. G. Lu, RSC
- 428 Adv., 2014, 4, 54268-54281.
- 429 (31) F. Liu, S. D. Lin, Z. Q. Zhang, J. W. Hu, G. J. Liu, Y. Y. Tu, Y. Yang, H. L. Zou, Y. M.
- 430 Mo, L. Miao, Biomacromolecules, 2014, 15, 968-977.
- 431 (32) L. Lu, Y. Zou, W. J. Yang, F. H. Meng, C. Deng, R. Cheng, Z. Y. Zhong,
- 432 Biomacromolecules, 2015, 16, 1726-1735.
- 433 (33) I. Hofmeister, K. Landfester, A. Taden, Macromolecules, 2014, 47, 5768-5773.
- 434 (34) Y. F. Zhang, Q. Yin, H. Lu, H. W. Xia, Y. Lin, J. J. Cheng, ACS Macro Lett., 2013, 2,
- 435 809-813.
- 436 (35) E. Uğuzdoğan, O. S. Kawasaki, Colloids Surf. A: Physicochem. Eng. Aspects, 2010, 368,
- 437 129-136.
- 438 (36) R. P. Johnson, Y. I. Jeong, J. V. John, C. W. Chung, D. H. Kang, M. Selvaraj, H. Suh, I.
- 439 Kim, Biomacromolecules, 2013, 14, 1434-1443.

- 440 (37) B. P. Bastakoti, S. Guragain, K. Nakashima, Y. Yamauchi, Macromol. Chem. Phys.,
- 441 2015, 216, 287-291.
- 442 (38) A. Santos, M. S. Aw, M. Bariana, T. Kumeria, Y. Wang, D. Losic, J. Mater. Chem. B,
- 443 2014, 2, 6157-6182.
- 444 (39) B. W. Liu, H. Zhou, S. T. Zhou, H. J. Zhang, A. C. Feng, C. M. Jian, J. Hu, W. P. Gao, J.
- 445 Y. Yuan, Macromolecules, 2014, 47, 2938-2946.
- 446 (40) S. Yamamoto, J. Pietrasik, K. Matyjaszewski, Macromolecules, 2008, 41, 7013-7020.
- 447 (41) Y. Pang, Q. Zhu, D. L. Zhou, J. Y. Liu, Y. Chen, Y. Su, D. Y. Yan, X. Y. Zhu, B. S. Zhu,
- 448 J. Polym. Sci.: Part A: Polym. Chem., 2011, 49, 966-975.
- 449 (42) S. Patra, E. Roy, P. Karfa, S. Kumar, R. Madhuri, P. K. Sharma, ACS Appl. Mater.
- 450 Interfaces, 2015, 7, 9235-9246.
- 451 (43) Y. Kang, Y. Ma, S. Zhang, L. S. Ding, B. J. Li, ACS Macro Lett., 2015, 4, 543-547.
- 452 (44) D. Schmaljohann, Adv. Drug Deliv. Rev., 2006, 58, 1655-1670.
- 453 (45) L. Sambe, K. Belal, F. Stoffelbach, J. Lyskawa, F. Delattre, M. Bria, F. X. Sauvage, M.
- 454 Sliwa, V. Humblot, B. Charleux, G. Cooke, P. Woisel, Polym. Chem., 2014, 5, 1031-1036.
- 455 (46) J. M. Zhuang, M. R. Gordon, J. Ventura, L. Y. Li, S. Thayumanavan, Chem. Soc. Rev.,
- 456 2013, 42, 7421-7435.
- 457 (47) M. Seleci, D. A. Seleci, M. Ciftci, D. O. Demirkol, F. Stahl, S. Timur, T. Scheper, Y.
- 458 Yagci, Langmuir, 2015, 31, 4542-4551.
- 459 (48) N. V. Tsarevsky, S. A. Bencherif, K. Matyjaszewski, Macromolecules, 2007, 40, 4439-
- 460 4445.
- 461 (49) H. Pohlit, I. Bellinghausen, M. Schömer, B. Heydenreich, J. Saloga, H. Frey,
- 462 Biomacromolecules, 2015, 16, 3103-3111.
- 463 (50) S. T. Sun, P. Y. Wu, Macromolecules, 2013, 46, 236-246.
- 464 (51) Z. S. Ge, S. Y. Liu, Macromol. Rapid Commun., 2009, 30, 1523-1532.

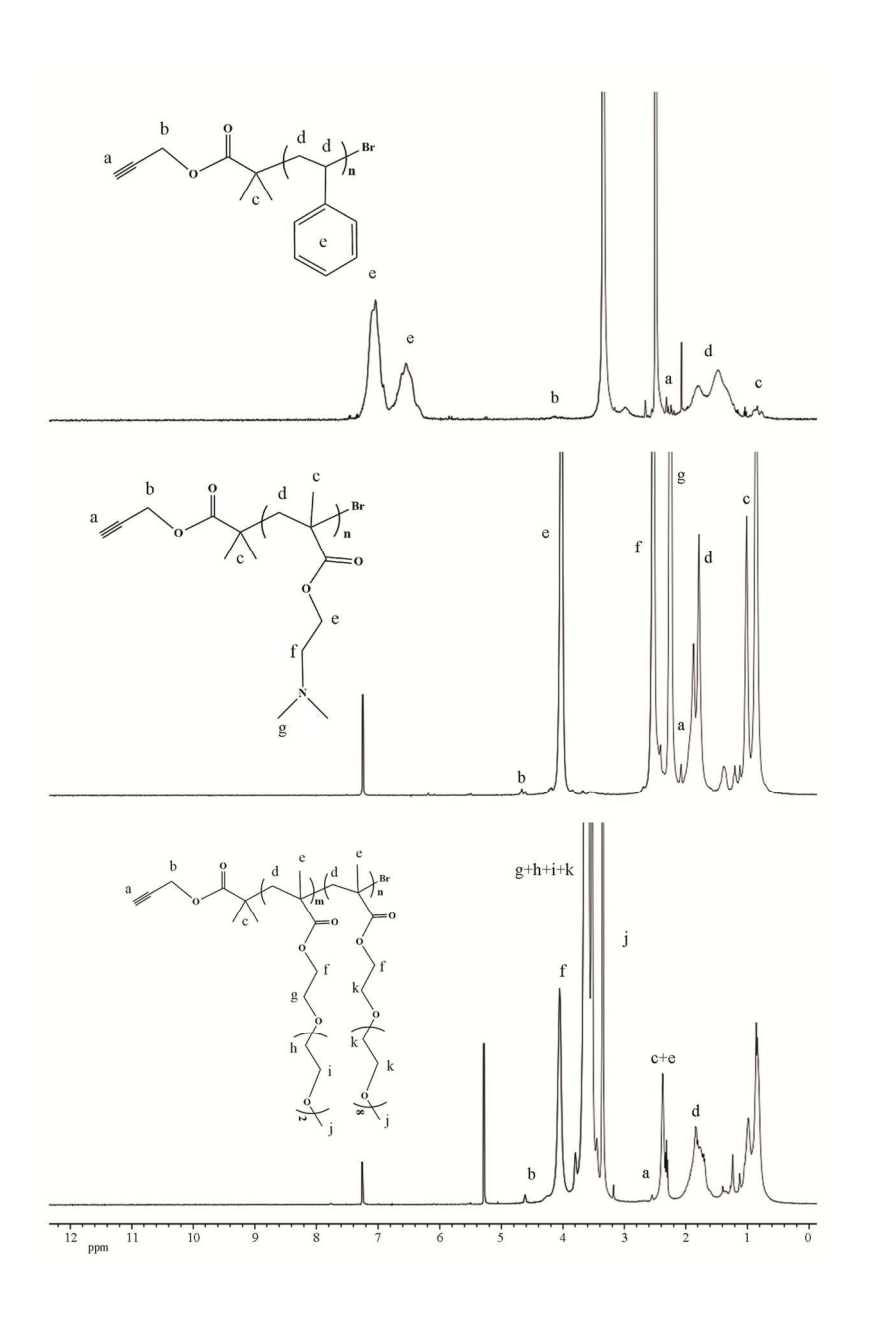
465 Figure captions

- 466 Fig. 1. The FT-IR spectra of MBIB, PGMA₅₀, (PGMA-N₃)₅₀, PDMAEMA-C≡CH, PS-C≡CH,
- 467 and POEGMA-C≡CH.
- 468 Fig. 2. The ¹H NMR spectra of PDMAEMA-C≡CH, PS-C≡CH, and POEGMA-C≡CH.
- 469 Fig. 3. The SEC traces of PDMAEMA-C≡CH, PS-C≡CH, and POEGMA-C≡CH and ternary
- 470 graft copolymer (TGC_1 and TGC_2).
- 471 Fig. 4. The FT-IR and ¹H NMR spectra for TGC₂.
- 472 Fig. 5. The fluorescent intensity (I_{395}/I_{385}) of pyrene $(6 \times 10^{-6} \text{ mol L}^{-1})$ changes with different
- 473 concentration of TGC₂ solutions and the critical micelle concentration (CMC).
- 474 Fig. 6. The micellar particle size distribution of TGC₂. (a) 20 °C and pH=7, (b) 40 °C and
- 475 pH=7, (c) 20 °C and pH=9, (d) 40 °C and pH=9.
- 476 Fig. 7. The typical TEM images of TGC₂. (a) 20 °C and pH=7, (b) 40 °C and pH=7, (c) 20 °C
- 477 and pH=9, (d) 40° C and pH=9.
- 478 Fig. 8. (a) Water; (b) Mixture of DOX and dichloromethane; (c) Adding water to the mixture
- of DOX/ dichloromethane; (d), and (e) Adding TGC aqueous solution (0.2 mg mL⁻¹, and 1 mg
- 480 mL⁻¹) to the mixture of DOX/ dichloromethane, respectively.
- 481 Fig. 9. Photographs of TGC₂ micelle solution (1 mg mL⁻¹, a) and TGC₂ micelle solution (1
- 482 mg mL⁻¹) loaded RB (b) and DOX (c), respectively.
- 483 Fig. 10. Release profiles of drugs loaded in TGC micelles. DOX+TGC₁ at pH=9.0 and 40 °C
- 484 (a); RB+TGC₁, Stage I : pH= 9 and 20 °C (b); RB+ TGC₁, Stage II : pH= 9 and 40 °C (c);
- 485 DOX + TGC₂ at pH=9.0 and 40 °C (d); RB+ TGC₂, Stage I : pH= 9 and 20 °C (e); RB+
- 486 TGC₂, Stage II: pH= 9 and 40 $^{\circ}$ C (f).
- 487 Scheme 1. Structure of PGMA-g-(PS-r-PDMAEMA-r-POEGMA).
- 488 Scheme 2. Synthetic routes toward PGMA-g-(PS-r-PDMAEMA-r-POEGMA).
- 489 Scheme 3 Molecular structures of Doxorubicin (DOX) and Rhodamine B (RB).

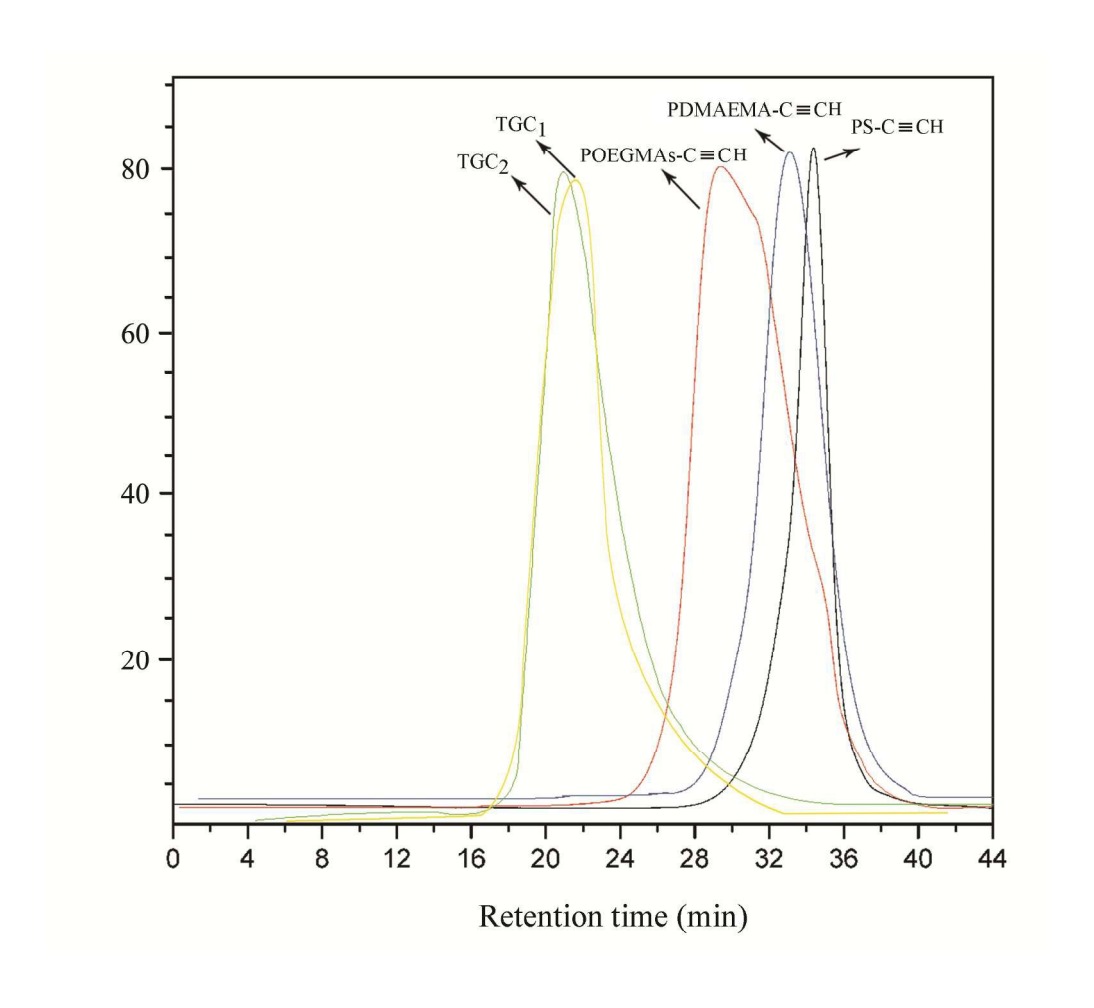
490	Scheme 4. Schematic illustrations of the dual thermo- and pH-induced self-assembly and
491	possible loading and release mechanism.
492	Graphfical abstract
493	Schematic illustrations of the self-assembly of TGCs and possible loading and release
494	mechanism



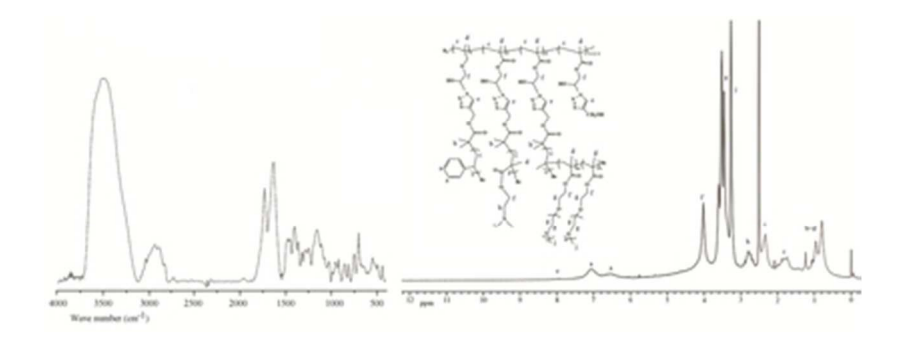
266x117mm (300 x 300 DPI)



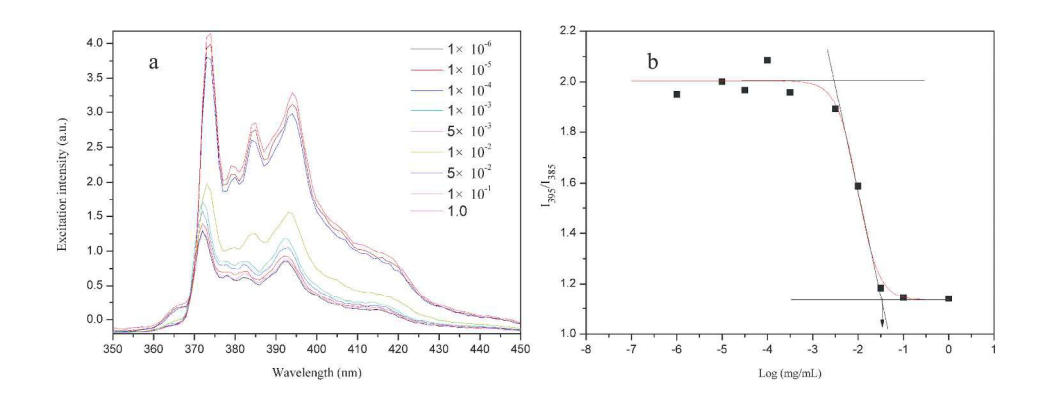
133x198mm (300 x 300 DPI)



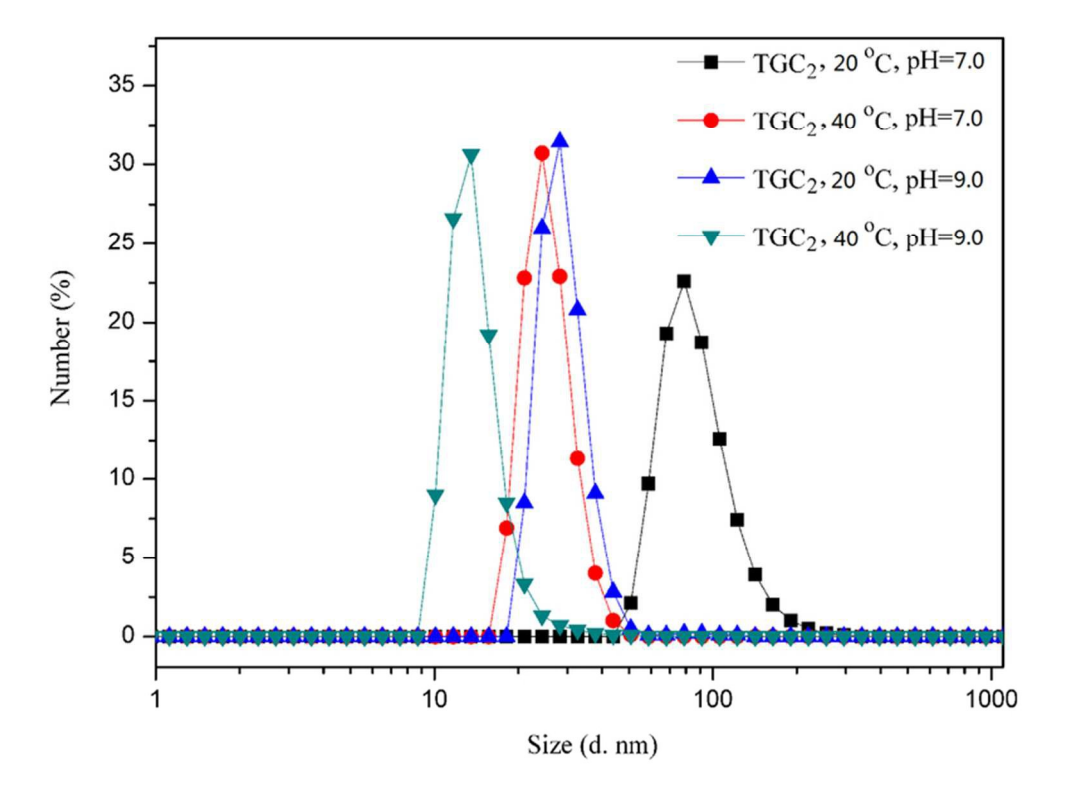
219x197mm (300 x 300 DPI)



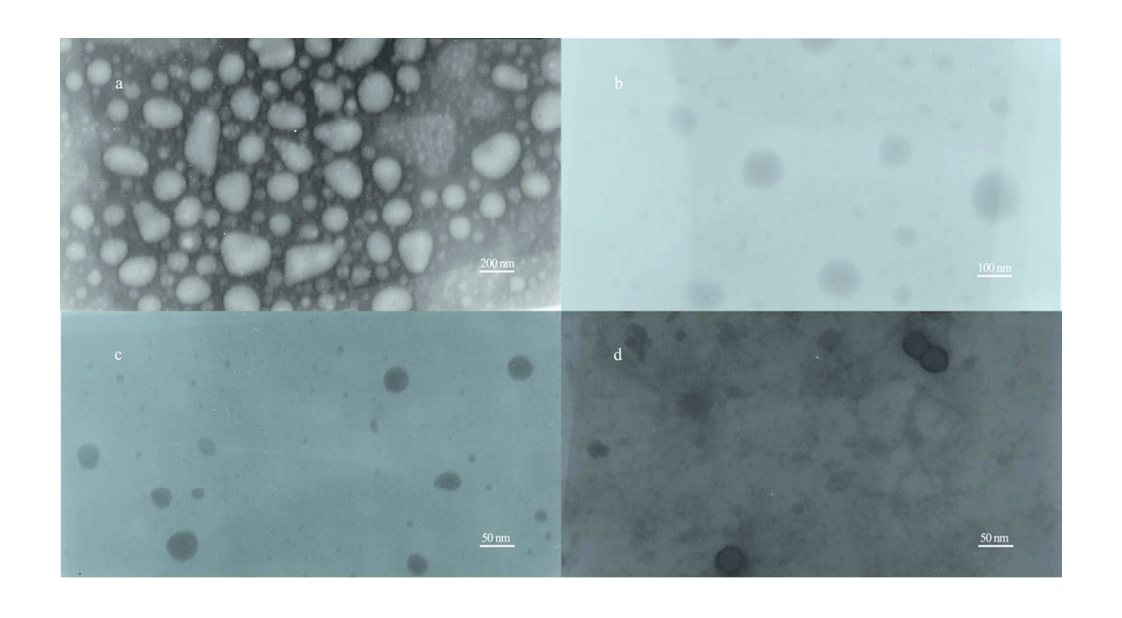
34x13mm (300 x 300 DPI)



279x108mm (300 x 300 DPI)



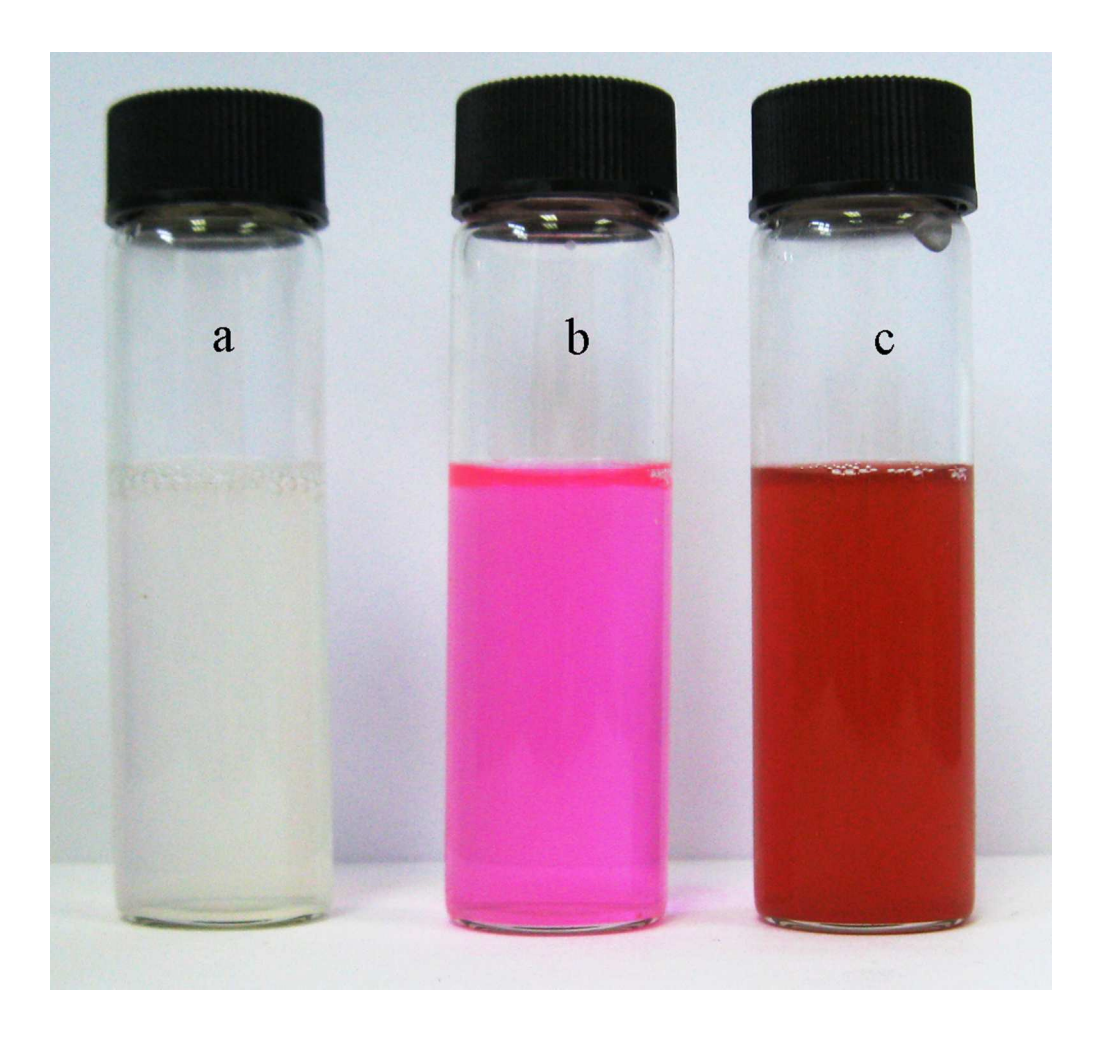
67x50mm (300 x 300 DPI)



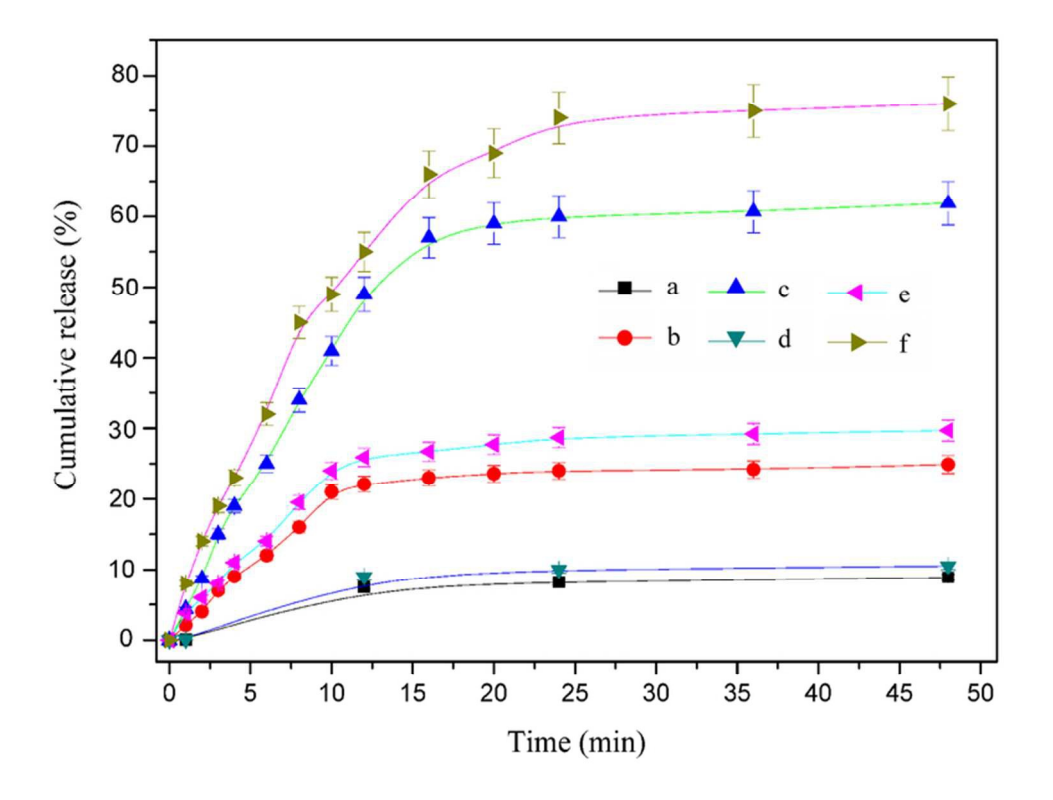
97x52mm (300 x 300 DPI)



60x41mm (300 x 300 DPI)



90x84mm (300 x 300 DPI)

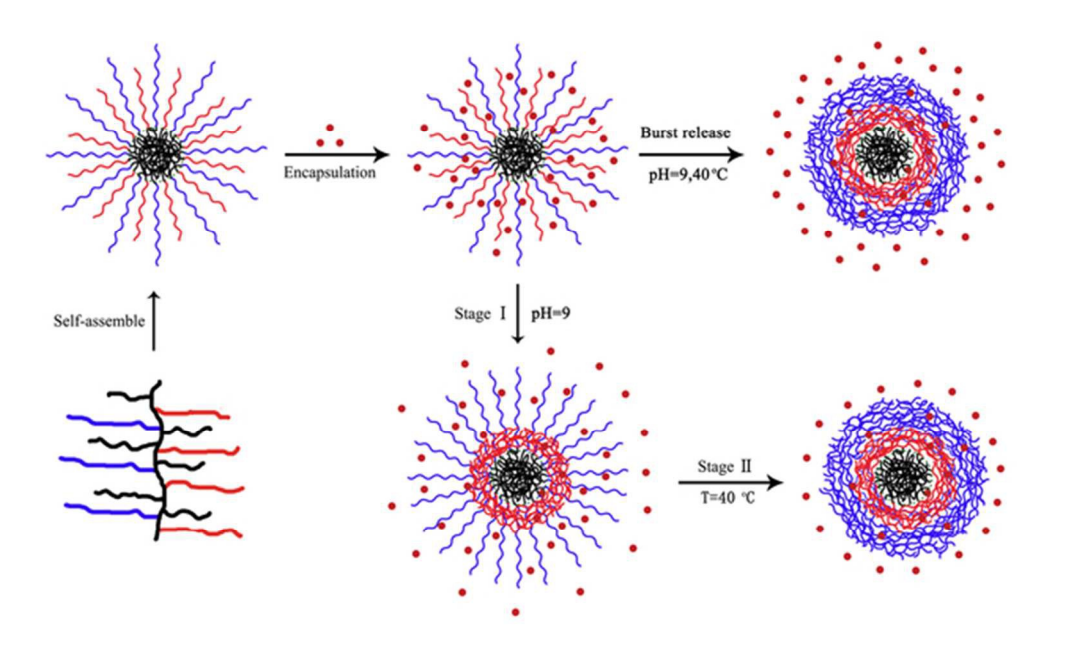


68x51mm (300 x 300 DPI)

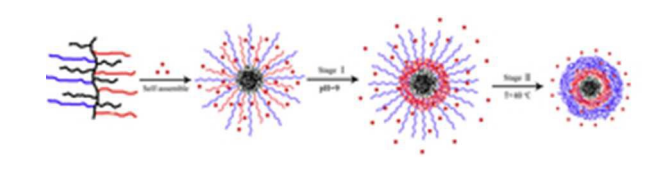
93x117mm (300 x 300 DPI)

152x128mm (300 x 300 DPI)

101x46mm (300 x 300 DPI)



53x32mm (300 x 300 DPI)



25x5mm (300 x 300 DPI)